COMPUTATIONAL MECHANICS 2023
38th conference with international participation
Srní
October 23 - 25, 2023

Measurement of paraphysiological strain in entire bones using digital volume correlation

P. Henyš[a], E. Dall'Ara[b], S. Martelli[c,d]

[a] Institute of New Technologies and Applied Informatics, Faculty of Mechatronics, Informatics and Interdisciplinary Studies, Technical University of Liberec, Liberec, Czechia
[b] Department of Oncology and Metabolism and INSIGNEO Institute for In Silico Medicine, University of Sheffield, Sheffield, UK
[c] Centre for Biomedical Technologies, School of Mechanical, Medical and Process Engineering, Queensland University of Technology, Brisbane, Australia
[d] Medical Device Research Institute, College of Science and Engineering, Flinders University, Tonsley SA, Australia

1. Introduction

(Para)physiological bone strain is critical for studying bone pathologies and related research. Digital Volume Correlation (DVC) provides experimental measurements of internal displacements and strains within the entire bone volume. DVC algorithms calculate a deformation map by maximizing a similarity metric in images of an object under two different deformation states. Among many other studies, DVC has been successfully used to study the deformation and fracture mechanism in the entire human femur [3] and the risk of fracture and bone adaptation in metastatic vertebral bodies [5, 6]. The present study quantifies the performance of Symmetric Normalization (SyN) [7] approach for studying the deformation of the human femur under subcritical loading relative to an established method for bone analysis, BoneDVC [1].

2. Methods

The downsampled microstructural images (voxel size: 0.12 mm) of the proximal half femur of a female donor (76 years of age, T-score: -2.12) were obtained at the Australian Synchrotron (Clayton VIC, Australia) during an earlier study [4]. The femur was imaged while subjected to no load and a hip contact force direction representing a static single-leg stance loading configuration whose amplitude caused high strain levels in the internal trabecular network and a localized trabecular collapse [3].

To estimate absolute registration error, a realistic bone displacement field was created synthetically and applied to the images of the undeformed femur using the finite element approach. To create the femur-specific finite-element model, the bone was segmented from the CT images using thresholding and morphometric operations to ensure the smoothness and continuity of the mask and converted into a mesh consisting of linear hexahedral elements. A linear elastic material for bone with a uniform modulus of 1 GPa and Poisson ratio 0.3 was considered. The femur was fully constrained distally. A vertical displacement of 1 mm was applied to a patch of nodes in the superior head of the femur of 1 cm in diameter. A cubic spline interpolation was used to warp the microstructural femur image with a computed displacement field. The displacement field was scaled by factors of 1 and 10, resulting in 2 different volumes with increasing synthetic displacement. Both BoneDVC and SyN were used to compute a map $\Delta(\bar{x})$ between the images of the femur undeformed and the set of images synthetically deformed. The strain error was defined as a difference between synthetic ε_{ref} and estimated ε

$$\delta\varepsilon := \varepsilon_{ref} - \varepsilon. \tag{1}$$

The strain was computed by projecting it onto a Discontinuous finite element space of zero-order. Considering coordinates $\bar{x}$ of reference image and image being registered x we can define a deformation map such $\Delta(\bar{x}) = x$ provided by SyN or BoneDVC. The displacement at the reference image can be expressed as $u(\bar{x}) = \Delta(\bar{x}) - \bar{x}$. Having displacement function defined on the reference domain, regularised projection of small-strain is employed in virtue of study [2]

$$\int_{\bar{\Omega}} \varepsilon : \delta r \, d\bar{\Omega} + \frac{a}{h} \int_{\partial\bar{\Omega}_e} [\varepsilon] : [\delta r] \, d\bar{s} = \frac{1}{2} \int_{\bar{\Omega}} (\nabla u + \nabla u^T) : \delta r \, d\bar{\Omega} \ , \ \delta r \ \forall V_{L2}. \tag{2}$$

The discontinuity across element interface was penalized with term containing 'jump' operator $[\cdot]$ and smoothing parameter α. Both algorithms consider the NS parameter, which gives the sampling density of the similarity metric for SyN [7] and the resolution of the numerical approximation for BoneDVC [1, 3]. The smoothing parameter α was set up to 10 or less based on zero-strain test [1, 3] and additional extensive numerical experiments. This value allows for keeping strain random error (SDER) under 500 microstrains [3].

3. Results

The highest strain errors were found concentrated in regions with smaller strain amplitudes. While SyN produced notably larger strain errors in regions with lower strains, they were relatively low and homogeneously distributed elsewhere (Fig. 1). The grid size parameter NS affected the strains estimated with BoneDVC more than the strain estimated with SyN. The error in the strain depends rather weakly on the strain amplitude. Observing the spatial distribution of strain errors, SyN generated localized errors in the femoral head and in the distal region of the femur whereas BoneDVC produced the largest error in the femoral head region (Fig. 2).

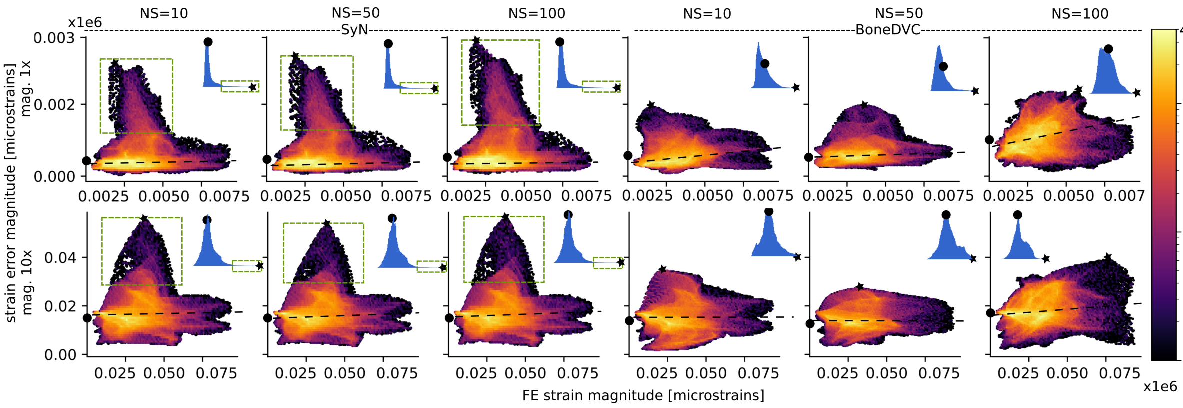

Fig. 1. The strain error dependence on imposed strain for different algorithms setups and magnitude levels. The scalar map displays the number of nodes with similar errors (frequency). A yellow color indicates a high concentration of errors with comparable values (high frequency), while a dark color signifies a low concentration (low frequency). Each line demonstrates the errors for different magnitude levels. The columns describe the sampling density of similarity metrics in the calculation. Blue histograms show error distributions with highest error marked as a black 'star' in both histograms and scatter plots. Dashed curve represents a curve estimated with linear regression. Green dashed boxes border abnormally high error peak regions located in lower amplitude regimes. Black circles represent the median of the error

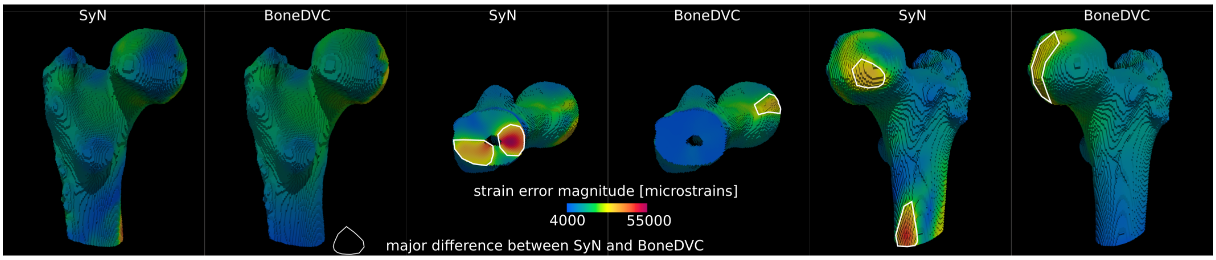

Fig. 2. Major differences in error distribution for strain computed with NS $= 10$ voxels and magnitude $=$ 10 mm. There are different views of the proximal femur on the left and right

Estimation of the displacement by SyN on a finer mesh showed a strongly localized deformation in the upper part of the femur at the point of contact with the loading device, with maximum displacement equal to 2.1 mm (Fig. 3). This value is closest to the displacement of the actuator (2.66 mm) measured in the images (sample #2, from [3]). The strain map in the SyN results displayed high focal strain in correspondence of a local collapse on the internal trabeculae which was visible earlier only in the full resolution images (0.03 mm voxel size) using BoneDVC [3].

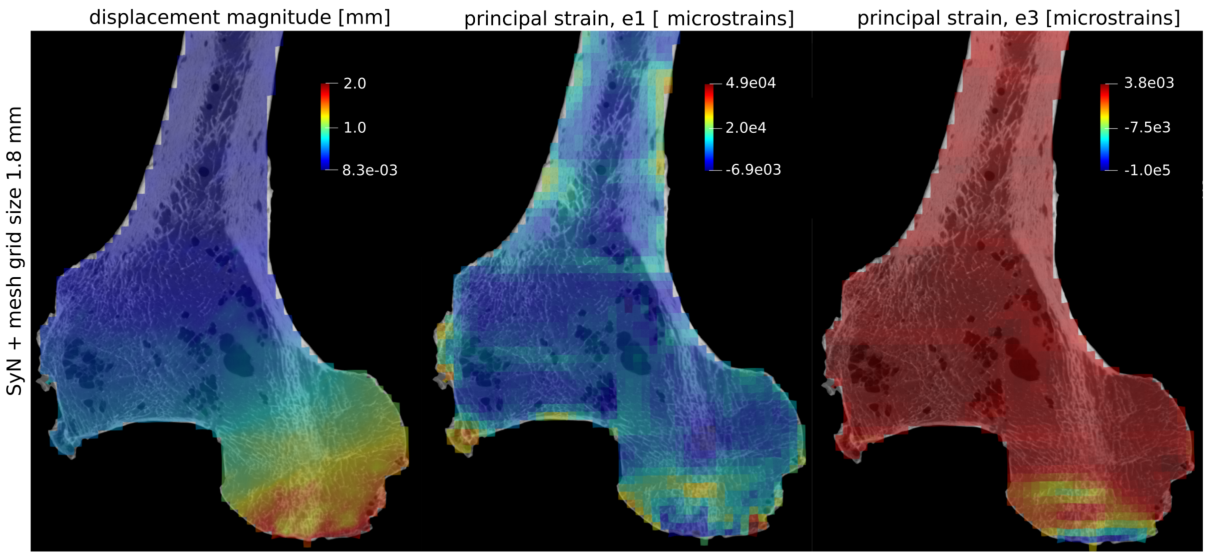

Fig. 3. Displacement and strain of femur under load computed with SyN with sampling rate NS $= 50$

4. Discussion

The errors in strain of two DVC approaches have been examined in a synthetic realistic displacement calculated using finite element simulation. In summary, it was found that:

- SyN provided a comparable solution to BoneDVC, although the error distribution differed either in terms of location and peak error.
- BoneDVC, in comparison, produces highly accurate strain predictions provided that the nodal spacing NS is carefully chosen balancing accuracy and computational time.
- The assessment of the absolute error should against a realistic deformation of reference allow to calibrate the smoothing parameter for noise suppression while preserving the localized features of the strain field.

Displacement and strain accuracy can be enhanced through smoothing. Generally, the range of values of α can be from zero to infinity, but in practice, the working range is much more narrow and it depends on deformation heterogeneity, mesh size and noise. It is worth noting that the smoothing effect can be partially controlled by BoneDVC's nodal resolution NS [1]. This effect was not observed in SyN where NS primarily influences computation time, but not accuracy. In fact, considering NS equal to 100 voxels resulted in a four-fold reduction in computational time, while maintaining accuracy comparable to NS equal to 1 voxel.

The error in the strain increases slightly with the strain amplitude. There are significant dispersions in the strain errors (especially in the lower strain regions for SyN). These deviations are caused locally and depend on the type of algorithm (i.e., SyN vs. BoneDVC) and also on the setup. Both used DVC methods are non-linear and thus the number of iterations and the numerical accuracy setting significantly affect the ability to correctly compute fine local strain. In both algorithms, these parameters were chosen optimally with respect to computational time.

While BoneDVC uses the optical flow equations to find the continuous deformation, SyN parameterizes the deformation map using sets of solutions of ODEs with uniquely defined initial conditions [7]. In both approaches, some type of additional regularisation is considered to ensure or improve the smoothness of the deformation map $\Delta(x)$. SyN regularises the velocities [7]. In BoneDVC, NS is the key parameter that determines the quality of the estimation because it is the parameter that directly determines at what resolution the displacement is computed. In the case of SyN, this parameter influences the sampling of the similarity metric and, according to the results in this study, does not have a significant impact on accuracy.

References

[1] Dall'Ara, E., Barber, D., Viceconti, M., About the inevitable compromise between spatial resolution and accuracy of strain measurement for bone tissue: A 3D zero-strain study, Journal of Biomechanics 47 (12) (2014) 2956-2963.

[2] Henyš, P., Vořechovský, M., Stebel, J., Kuchař, M., Exner, P., From computed tomography to finite element space: A unified bone material mapping strategy, Clinical Biomechanics 97 (2022) No. 105704.

[3] Martelli, S., Giorgi, M., Dall' Ara, E., Perilli, E., Damage tolerance and toughness of elderly human femora, Acta Biomaterialia 123 (2021) 167-177.

[4] Martelli, S., Perilli, E., Time-elapsed synchrotron-light microstructural imaging of femoral neck fracture, Journal of the Mechanical Behavior of Biomedical Materials 84 (2018) 265-272.

[5] Palanca, M., Cavazzoni, G., Dall'Ara, E., The role of bone metastases on the mechanical competence of human vertebrae, Bone (2023) No. 116814.

[6] Palanca, M., De Donno, G., Dall'Ara, E., A novel approach to evaluate the effects of artificial bone focal lesion on the three-dimensional strain distributions within the vertebral body, Plos ONE 16 (6) (2021) No. e0251873.

[7] Tustison, N. J., Cook, P. A., Holbrook, A. J., Johnson, H. J., Muschelli, J., Devenyi, G. A., Duda, J. T., Das, S. R., Cullen, N. C., Gillen, D. L., Yassa, M. A., Stone, J. R., Gee, J. C., Avants, B. B., The ANTsX ecosystem for quantitative biological and medical imaging, Scientific Reports 11 (1) (2021) No. 9068.